ACCEPTED VERSION

Whittall, J.J.; Morona, R.; Standish, A.J.
Topology of Streptococcus pneumoniae CpsC, a polysaccharide co-polymerase and BY-kinase adaptor protein, *Journal of Bacteriology*, 2015; 197(1):120-127

Copyright © 2015, American Society for Microbiology. All Rights Reserved.

PERMISSIONS

http://journals.asm.org/site/misc/ASM_Author_Statement.xhtml

Authors may post their articles to their institutional repositories
ASM grants authors the right to post their accepted manuscripts in publicly accessible electronic repositories maintained by funding agencies, as well as appropriate institutional or subject-based open repositories established by a government or non-commercial entity. Since ASM makes the final, typeset articles from its primary-research journals available free of charge on the ASM Journals and PMC websites **6 months after final publication**, ASM recommends that when submitting the accepted manuscript to PMC or institutional repositories, the author specify that the posting release date for the manuscript be no earlier than 6 months after the final publication of the typeset article by ASM.

16 February 2015

http://hdl.handle.net/2440/88961

JB Accepts, published online ahead of print on 13 October 2014
J. Bacteriol. doi:10.1128/JB.02106-14
Copyright © 2014, American Society for Microbiology. All Rights Reserved.

JB Accepts published online ahead of print

1

2

3 **Topology of *Streptococcus pneumoniae* CpsC, a Polysaccharide co-polymerase and BY-**

4 **kinase adaptor protein**

5

6 **Running title: CpsC C-terminus is extracytoplasmic**

7

8 **Jonathan J. Whittall, Renato Morona and Alistair J. Standish[#]**

9

10

11 School of Molecular and Biomedical Sciences, University of Adelaide, SA, Australia.

12

13

14 # Address correspondence to: Alistair Standish (alistair.standish@adelaide.edu.au)

15

JB Accepts published online ahead of print

16 **Abstract**

17 In Gram-positive bacteria, tyrosine kinases are split into two proteins, the cytoplasmic
18 tyrosine kinase and a transmembrane adaptor protein. In *Streptococcus pneumoniae* this
19 transmembrane adaptor is CpsC, with the C-terminus of CpsC critical for interaction and
20 subsequent tyrosine kinase activity of CpsD. Topology predictions suggest CpsC has two
21 transmembrane domains, with the N and C-termini present in the cytoplasm. In order to
22 investigate CpsC topology, we used a chromosomal HA-tagged Cps2C protein in D39.
23 Incubation of both protoplasts and membranes with the CP-B resulted in complete
24 degradation of HA-Cps2C in all cases, indicating that the C-terminus of Cps2C was likely
25 extra-cytoplasmic, and hence the protein's topology was not as predicted. Similar results
26 were seen with membranes from TIGR4, indicating Cps4C also showed similar topology. A
27 chromosomally encoded fusion of HA-Cps2C and Cps2D was not degraded by CP-B,
28 suggesting that the fusion fixed the C-terminus within the cytoplasm. However, capsule
29 synthesis was unaltered by this fusion. Detection of the CpsC C-terminus by flow cytometry
30 indicated that it was extra-cytoplasmic in approximately 30% of cells. Interestingly, a mutant
31 in the protein tyrosine phosphatase CpsB had a significantly greater proportion of positive
32 cells, although this affect was independent of its phosphatase activity. Our data indicate that
33 CpsC possesses a varied topology, with the C-terminus flipping across the cytoplasmic
34 membrane where it interacts with CpsD in order to regulate tyrosine kinase activity.

35

36

JB Accepts published online ahead of print

37 **Introduction**

38

39 The critical importance of bacterial tyrosine phosphorylation to the basic physiology and
40 virulence of a wide range of pathogens is becoming increasingly more recognized (1). This
41 has led to investigation of bacterial protein tyrosine phosphatases and tyrosine kinases (BY-
42 kinases) as novel targets for the development of antimicrobials (2, 3). *Streptococcus*
43 *pneumoniae* is one such human pathogen for which tyrosine phosphorylation is critical. In the
44 pneumococcus, tyrosine phosphorylation plays an important role in regulation of the
45 biosynthesis of the polysaccharide capsule. The capsule is considered the major virulence
46 factor of the pneumococcus, through its ability to act as an anti-phagocytic factor (4), and
47 indeed all isolates causing invasive disease are encapsulated.

48

49 In recent times, we have investigated the role of a tyrosine phosphoregulatory system in the
50 regulation of the biosynthesis of the polysaccharide capsule. The three genes responsible for
51 this system are co-transcribed at the 5' end of the capsule locus, with all being essential for
52 the complete encapsulation of the pneumococcus (5-8). These three genes are responsible for
53 encoding a protein tyrosine phosphatase (CpsB) (6) which acts to dephosphorylate an auto-
54 phosphorylating bacterial tyrosine kinase CpsD (BY-kinase), along with the polysaccharide
55 co-polymerase protein (PCP) CpsC (7). While in Gram-negative bacteria BY-kinases are
56 present as one single protein, in Gram-positive bacteria they are comprised of two separate
57 co-transcribed proteins which are required for kinase activity (7, 9). In the pneumococcus,
58 this adaptor protein is CpsC. CpsD forms the active tyrosine kinase, possessing the Walker A
59 and B motifs, as well as the tyrosines present at its C-terminus which are trans-
60 autophosphorylated by another CpsD monomer (9). However, CpsC is required for this
61 tyrosine kinase activity, likely through its ability to enable the binding of ATP based on

JB Accepts published online ahead of print

62 studies of the *Staphylococcus aureus* homologs (9), and thus absence of CpsC results in a
63 lack of detectable CpsD auto-phosphorylation (7, 10).
64
65 CpsC is a member of the 2b sub-family of PCPs (11). In Gram-negative bacteria, PCP
66 proteins are associated with regulating O-antigen chain length during O-antigen
67 polymerization and synthesis of type 1 capsules and exopolysaccharides (8, 11). Previous
68 work undertaken in our laboratory has suggested CpsC is critical for the attachment of
69 capsule to the cell wall (12), while a number of amino acid substitutions in this large extra-
70 cytoplasmic loop significantly reduced phosphorylation of the BY-kinase CpsD (13). This
71 suggests that there is a signal which can be transmitted across the cytoplasmic membrane to
72 or from this extracellular loop which affects CpsD BY-kinase activity. However, the nature
73 of this signal and its transmission is still unknown.
74
75 In this study, we investigated the topology of CpsC to provide insight into the mechanism for
76 CpsC activation of CpsD. Unexpectedly, using a variety of methods, and in two different
77 strains, we discovered that the C-terminus of CpsC has varied topology, with it being both
78 intra- and extra-cytoplasmic. We suggest that this novel CpsC topology may be critical in its
79 ability to regulate CpsD tyrosine kinase activity, and thus regulate encapsulation of this major
80 human pathogen.
81

JB Accepts published online ahead of print

82 **Materials and Methods**

83 **Growth Media and Growth conditions**

84 *S. pneumoniae* D39, and TIGR4 were grown in Todd-Hewitt broth with 1% Bacto yeast
85 extract (THY), or on blood Agar. Broth cultures were grown at 37 °C without agitation.
86 *Escherichia coli* strains were grown in Luria-Bertani broth (10g/L Tryptone, 5 g/L yeast
87 extract, 5 g/L NaCl) broth or agar, with transformation carried out using $CaCl_2$-treated cells.
88 Antibiotics used were as follows: Erythromycin (Ery): *S. pneumoniae* 0.2 µg/ml; Ampicillin
89 (Amp) 100 µg/ml.

90

91 **DNA Methods**

92 *E. coli* K-12 DH5α was used for all cloning experiments. DNA manipulation, PCR,
93 transformation and electroporation was performed as previously described
94 (14). Oligonucleotide sequences are available on request.

95

96

97

98 **Production of StrepTagII-Cps4CD**

99 A fusion protein comprising the last 29 aa's of Cps4C (the predicted cytoplasmic region) with
100 the entire Cps4D protein was constructed by overlap extension PCR. First, the coding
101 sequence for the CpsC C-terminus without its stop codon was amplified using AS1/AS2, and
102 the coding sequence for the CpsD protein was amplified with AS3/AS4 using DNA from
103 TIGR4 *S. pneumoniae* as template. A second round of PCR with AS1/AS4 stitched these
104 products together. This PCR was then digested with *Kpn*I and *Sac*I, restriction sites for which
105 were included in primers AS1/AS4. This digested PCR product was then ligated into likewise
106 digested pTRIEX6 to generate a StrepTagII-Cps4CD construct. This ligation was then

JB Accepts published online ahead of print

107 transformed into DH5α, screened by PCR, with the correct plasmid confirmed by sequencing
108 (pTRIEX6-Cps4CD). pTRIEX6-Cps4CD was isolated and then transformed into Lemo21
109 (DE3) (15) for protein over-expression, yielding strain AS35.
110 For over-expression, strains were grown at 37 °C for 16 h in LB, subcultured 1/20 into fresh
111 broth and grown for another 2 hr to an OD_{600} of ≈ 0.5. Strep-TagII-Cps4CD expression was
112 then induced by addition of 1 mM IPTG for further 2 h. The bacteria were pelleted, and the
113 cells disrupted using a Constant Systems cell disruptor. The soluble recombinant StrepTagII-
114 Cps4CD was then purified using an AKTA prime plus (GE Life Sciences) with a StrepTrap
115 (GE Healthcare Life Sciences) as per manufacturer's instructions, resulting in the purification
116 of approximately 2 mg/ml CpsCD. Protein was then supplied to IMVS, Veterinary Services,
117 Gilles Plain SA, Australia where polyclonal rabbit serum was produced, designated αCpsCD.
118
119 **Construction of strain D39EHA:CpsC-L11-CpsD and D39CpsB$_{H136A}$**
120 A strain was constructed which comprised Cps2C fused to Cps2D with a linker (L11) based
121 on a previous study using a different pneumococcal serotype (16). The initial rounds of PCR
122 amplified *cps2C* with linker (Cps5' + AS 169) and *cps2D* with linker AS168 + AS159, using
123 D39EHA:Cps2C chromosomal DNA. These products were then combined in a second round
124 of PCR with oligonucleotides Cps5' + AS159. Transformation and selection were performed
125 as described previously (17), and transformed colonies were screened by PCR and DNA
126 sequencing.
127 In order to construct a point mutation in CpsB which inactivated its phosphatase activity, we
128 constructed D39CpsB$_{H136A}$ based on a recent study(18). Originally, a strain (D39cpsJANUS)
129 was constructed with the janus cassette (19) inserted in place of *cpsB*, *cpsC* and *cpsD*. In
130 order to do this, first the janus cassette was amplified with oligonucleuotides AS113 and
131 AS114 along with flanking regions upstream (AS115 + Cps5') and downstream (AS116 +

JB Accepts published online ahead of print

132 AS159) of *cpsBCD*. The three PCRs were then combined in a second round of PCR with
133 Cps5' and AS 159. This was then transformed into streptomycin resistant D39.
134 Oligonucleotides AS262 + AS159, and AS263 + Cps5' were then used to amplify *cps2B*
135 from D39 *S. pneumoniae* encoding the relevant change. The PCRs were combined by a
136 second round of PCR using AS159 + Cps5' and then this PCR was then transformed into
137 D39cpsJANUS. The relevant mutation was confirmed by DNA sequencing.
138
139 **Western Immunoblotting**
140 Insoluble fractions, protoplasts, and whole cell lysates were separated on 12% SDS-PAGE
141 and transferred to Nitrobind (GE Water and Process technologies). In order to investigate the
142 presence of smaller digested products, insoluble fractions were separated on 16.5% Mini-
143 PROTEAN Tris Tricine Gels (Biorad) according to the manufacturer's instruction, prior to
144 Western immunoblotting. Membranes were probed with primary antibody overnight (αHA
145 (Sigma Aldrich; #H3663) 1/2500, or αCpsCD (1/1000), αPY (4G10, Bio X Cell; #BE0194)
146 and after washing, incubated with either goat anti-rabbit or goat anti-mouse secondary
147 antibodies (Biomediq DPC) for 2 h. Detection was performed with chemiluminescence
148 blotting substrate (Sigma Aldrich) as per manufacturer's instructions. Benchmark prestained
149 molecular weight markers (Life Technologies) were used as molecular size markers.
150 Stripping of western immunoblots was performed by incubation with Restore PLUS Western
151 Blot Stripping buffer (Thermo Scientific).
152
153 **Protoplast formation**
154 Pneumococci were grown to OD_{600} = 0.5 in THY at 37 °C, washed twice in 300 μL
155 phosphate buffered saline (PBS), followed a single wash in 250 μL of 0.05 mM EDTA, pH
156 8.0. Pellets were resuspended in 300 μL mutanolysin solution (20 mM Tris-HCl (Amresco)

JB Accepts published online ahead of print

157 pH 6.8, 0.1 mM $MgCl_2$, 10 U/mL mutanolysin (Sigma Aldrich), 40 % (w/v) sucrose) before
158 incubation for 3 h at 37 ˚C. Protoplasts were washed twice in 200 µL 40 % (w/v) sucrose
159 PBS solution, with confirmation of protoplast formation by phase contrast microscopy.
160
161 **Isolation of membrane containing fractions**
162 *S. pneumoniae* cultures were harvested at 17000 × *g* for 30 mins. Pellets were resuspended in
163 10 mL resuspension buffer (RB) (100 mM Tris-HCl pH 7.4, 200 mM NaCl, 20% glycerol)
164 with 100 µL 100x Protease Arrest (Gbiosciences) and 5 mM EDTA. Bacterial suspensions
165 were lysed at > 1000 PSI via a French pressure cell. Cell debris was removed at 20,000 × *g*
166 for 50 mins. Pellets containing bacterial membranes were isolated from the supernatant by
167 ultra-centrifugation at 150,000 × *g* for 1 h. Pellets were then washed 3 × in 50 mL RB before
168 resuspension in ~100 µL RB, after which total membrane was quantified using BCA Protein
169 Assay (Pierce).
170
171 **Carboxypeptidase B accessibilty assays**
172 Carboxypeptidase B (CP-B) (Sigma Aldrich) analysis was conducted according to
173 manufacturer instructions. In brief, CP-B digestion was conducted in a 20 µL of 25 mM Tris-
174 HCl pH 7.65, 200 mM NaCl at 25 °C for 1 h. 1 $mg.mL^{-1}$ of total bacterial membrane protein
175 or 10 µL of protoplasts were used in all assays. In order to identify degradation products, the
176 reaction size was increased to 1 ml, and following CP-B digestion, membranes were isolated
177 by ultra-centrifugation at 150,000 × *g* for 1hr and subsequently analysed by SDS-PAGE and
178 Western immunobloting. Protoplast CP-B analysis occurred in 40% (w/v) sucrose to prevent
179 cell lysis. CP-B reactions were stopped after 1 h by the addition of 2 µL of a 10x Protease
180 Arrest, 50 mM EDTA solution. Samples were then analysed by Western immunoblotting.
181 Cps2C-L11-Cps2D fusion protein was extracted from 8 $mg.mL^{-1}$ D39EHA:Cps2C-L11-

JB Accepts published online ahead of print

182 Cps2D membranes by solubilization in 0.5 % (w/v) DDM for 1 hr at 25 °C. The remaining
183 insoluble membrane and protein was then removed by ultra-centrifugation at 150,000 × *g* for
184 1hr, before incubation of the solubilized protein with CP-B.
185
186 **Flow cytometric analysis**
187 Flow cytometric analysis was carried out on bacterial protoplasts as prepared above.
188 Protoplasts were fixed in PBS with 25 % (w/v) NaCl, 3.7 % (v/v) formaldehyde for 20
189 minutes and washed in PBS with 40 % (w/v) sucrose. The cells were blocked in PBS with 40
190 % (w/v) sucrose, 10 % (v/v) fetal calf serum, and then with primary rabbit α-CpsCD
191 antibody (1/50) for 3 h. Following 3 washes in PBS with 40 % (w/v) sucrose, protoplasts
192 were incubated with secondary Alexa Fluor 488 nm donkey-α-rabbit (Life Technologies)
193 antibody for 1 h. Following 3 washes in PBS with 40 % (w/v) sucrose, flow cytometric
194 analysis of the labelled pneumococcal protoplasts (≥10,000 events) was then performed on
195 the bacterial protoplasts using a BD FACSCanto (Becton Dickinson Biosciences) cell
196 analyzer, with excitation laser at 488 nm, and emission captured using the FITC 530/30 filter.
197 Baseline fluorescence was calibrated using secondary antibody only. Analysis was performed
198 by FlowJo. Cells were calculated as positive in relation to a negative control which had only
199 the secondary antibody.
200
201 **Uronic Acid Assay**
202 The quantitative uronic acid assay was undertaken essentially as described previously (2, 12).
203 Levels were related back to a standard curve of D-glucuronic acid (Sigma).
204

JB Accepts published online ahead of print

205 **Results**

206 **Topology predictions of CpsC**

207 While topology investigations of PCP proteins have been undertaken, the PCP 2b subfamily
208 has so far been neglected. The predicted topology of Cps2C is shown in **Figure 1**. To predict
209 this topology we have analysed this protein with the following topology programs,
210 SPOCTOPUS (20), TOPSCONS (21), TMpred(22), and Philius (23) all with similar results.
211 Cps2C was predicted to have two transmembrane domains with the N and C-terminus in the
212 cytoplasm. The large extra-cytoplasmic loop is thought to contain a series of alternating α-
213 helices and β-strands (24). We were thus interested if these predictions were accurate and set
214 out to investigate the topology of CpsC.

215

216 **CP-B cleaves Cps2C and Cps4C in pneumococcal membranes**

217 We initially investigated the topology of Cps2C using CP-B accessibility assays. CP-B is a
218 C-terminal peptidase with a propensity for basic amino acids, of which there are a substantial
219 number at the C-terminal end of CpsC. Previously, this has been used successfully to
220 investigate the topology of related PCP proteins (25). CP-B was expected to cleave Cps2C
221 until it met the cell membrane. Using this method, we therefore expected we would be able to
222 determine the orientation and size of the predicted C-terminal cytoplasmic region. In previous
223 work, we constructed a strain which expressed Cps2C fused to a HA tag at its N-terminus
224 (13). We reasoned this would allow identification of cleavage products, as αHA recognizes
225 its epitope at the N-terminus of the protein.

226

227 We undertook CP-B cleavage assays using membrane fractions of D39EHA:Cps2C.
228 Following incubation with the protease, the fractions were separated on SDS-PAGE, and
229 Western immunoblotting undertaken, probing with an antibody against the HA tag to detect

JB Accepts published online ahead of print

230 HA-Cps2C. Using this method we saw significant degradation of Cps2C by CP-B (**Figure**
231 **2A & 2B**). However, there was no evidence of smaller degradation products. The predicted
232 transmembrane region should have stopped CP-B cleavage, resulting in degradation products
233 of significant size, and enabling estimation of the size of the cytoplasmic C-terminus. As the
234 predicted cytoplasmically located C- terminus of Cps2C has a predicted molecular weight of
235 4.6 kDa (Expasy), we would have expected to identify a protein that was approximately 24
236 kDa. In order to investigate if CP-B was simply degrading all proteins, we separated the
237 proteins from CP-B treated membranes by SDS-PAGE and stained the proteins with
238 Coomassie Brilliant Blue (**Figure 2C**). Few proteins showed any obvious degradation,
239 suggesting that the CP-B cleavage of HA-Cps2C detected was not due to a non-specific
240 degradation of all protein. Thus, this led to the hypothesis that the topology of Cps2C was not
241 as predicted in **Figure 1**.

242 In an effort to detect smaller degradation products, we increased the reaction size and
243 optimised the Western blotting procedure as described in Materials and Methods. A band of
244 approximately 9 kDa was evident when we digested with CP-B (Figure 2D), with its intensity
245 increasing with increasing CP-B concentration. Interestingly, this correlated with the
246 approximate size of the N-terminus along with its predicted trans-membrane domain (8.1
247 kDa; Expasy). This suggested that CpsC possesses one and not two transmembrane regions.

248 In order to investigate whether CP-B degradationoccurred across serotypes, we investigated
249 cleavage of Cps4C from TIGR4. As Cps4C and Cps2C share significant homology (78%
250 Identity), they are predicted to have similar topologies. As this strain did not possess a HA-
251 Cps4C, initially, αCpsCD, produced as described in Materials and Methods was used to
252 probe *E. coli* expressed StrepTagII-Cps4C in a Western immunoblot, and a band of the
253 expected size was detected indicating that this antibody recognized *S. pneumoniae* Cps4C
254 (**Figure 3A**). The only region in common between CpsCD (the protein used to produce the

JB Accepts published online ahead of print

255 antibody) and Cps4C is epitopes corresponding to the C terminal 29 aa of Cps4C. Thus, we
256 used this antibody to probe CP-B degradation of Cps4C in *S. pneumoniae* TIGR4
257 membranes. Insoluble membrane fractions were used such that the antibody could not
258 recognize Cps4D, which is a soluble cytoplasmic protein, and has been shown previously to
259 not be present in membrane fractions (7). TIGR4 membrane fractions were incubated with
260 CP-B, and subsequently analyzed for cleavage by Western immunoblotting, probing with
261 αCpsCD. With *S. pneumoniae* TIGR4 membranes, significant degradation of Cps4C was
262 detected (**Figure 3B & 3C**), with almost complete degradation seen with 100 μg/ml CP-B.
263 Thus, this suggested that these proteins did indeed share similar topology.
264
265 **Cps2C is cleaved in D39EHA:Cps2C pneumococcal protoplasts**
266 In order to investigate this further we performed CP-B cleavage on D39EHA:Cps2C
267 protoplasts. Cleavage would only be expected to occur if the C-terminus was extra-
268 cytoplasmic, as the protease should not enter the cell. Interestingly, significant cleavage of
269 Cps2C was also evident here (**Figure 4A and 4D**). As a control to ensure CP-B did not enter
270 the cell, we stripped the Western immunoblot and re-probed with anti-CpsCD which while it
271 recognizes CpsC when used at high concentrations, predominantly recognizes CpsD (as seen
272 by the size difference between the bands in **Figure 4A and 4B**). This showed CpsD was not
273 cleaved (**Figure 4B).** Additionally, this also showed that there were not a significant
274 proportion of cells lysing during the protoplast process which would account for the
275 degradation of Cps2C. However, when lysed D39 protoplasts were incubated with CP-B,
276 significant degradation of CpsD was evident (**Figure 4C**). Thus, this data suggested CP-B
277 could not traverse the protoplast cell membrane and enter the cytoplasm. This suggested that
278 the C-terminus of Cps2C was exposed to the external environment.
279 **D39HACpsC-L11-CpsD is not degraded by Carboxypeptidase B**

JB Accepts published online ahead of print

280 Henriques *et al.* (2011) (16) recently showed that fusion of CpsC and CpsD on the
281 chromosome resulted in a strain which was still encapsulated and regained tyrosine kinase
282 activity. We postulated that fusion of CpsC and CpsD would change the topology and
283 localization of CpsC, resulting in its C-terminus being fixed within the cytoplasm. Thus, we
284 constructed a fusion on the pneumococcal chromosome linking the two proteins via a linker
285 as previously described by Henriques *et al* (2011). This strain, D39EHA:Cps2C-L11-Cps2D
286 produced capsule to a similar level compared to the wildtype D39EHA:Cps2C strain (**Figure**
287 **5A**), which confirms previous findings (16). Furthermore, the strain produced an
288 approximately 52kdA protein (corresponding to the size of CpsC + CpsD + L11 + HA tag)
289 which reacted both with α-HA, α-CpsCD and also intensely with α-PY (4G10) indicative that
290 it was producing an active tyrosine kinase protein, able to auto-phosphorylate on tyrosines at
291 its C-terminus (**Figure 5B**).
292
293 In order to investigate CpsC topology in this strain, we incubated both protoplasts and
294 insoluble protein fractions with CP-B. CP-B was unable to cleave Cps2C-L11-Cps2D when
295 it was incubated with either insoluble membrane fractions or protoplasts of D39EHA:Cps2C-
296 L11-Cps2D (**Figure 5C, 5D, 5E & 5F**). We confirmed CP-B was able to cleave this Cps2C-
297 L11-CpsD fusion by solubilizing the membrane protein out of the insoluble fraction and then
298 performing the CP-B cleavage (**Figure 5G)**. Thus, these results suggested that fusion of
299 CpsC to CpsD altered the topology of CpsC, although did not alter its activity in promoting
300 capsule biosynthesis.
301
302 **Flow Cytometry Analysis**
303 As described above, α-CpsCD recognizes both the C-terminal region of Cps4C, and Cps4D.
304 In order to show that it also recognized Cps2C, and specifically its C-terminus, we isolated

JB Accepts published online ahead of print

305 insoluble membrane fractions of D39EHA:Cps2C and D39EHA:CpsC$_{D202\Delta}$, a strain in which
306 the 28 C-terminal amino acids are deleted (13). As D39EHA:CpsC$_{D202\Delta}$ expresses
307 substantially less CpsC than D39EHA:Cps2C, we controlled for this by performing a
308 simultaneous Western immunoblot with αHA. While α-CpsCD recognized Cps2C in
309 D39EHA:Cps2C, no corresponding band was detected in D39EHA:CpsC$_{D202\Delta}$ (**Figure 6**). As
310 this assay was performed with denatured protein, it would be highly unlikely that the
311 antibody is not recognizing CpsC in D39EHA:CpsC$_{D202\Delta}$ due to the mutation affecting the
312 overall folding of the protein. Thus, this showed that α-CpsCD specifically recognizes the C-
313 terminus of Cps2C. Therefore, we decided to use this antibody in flow cytometry in order to
314 provide additional evidence that the C-terminus of CpsC was exposed to the environment.
315
316 Initially flow cytometry with αCpsCD was undertaken on whole cell pneumococci, however,
317 no signal was detected (data not shown). This was not surprising as the capsular
318 polysaccharide present on the outside of the cell likely shields the C-terminus of Cps2C.
319 Therefore, we made protoplasts and undertook the flow cytometric analysis as described in
320 Materials and Methods. D39 wt protoplasts reacted well, with approximately 30% of cells
321 being positive (**Figure 7A, 7B**). Conversely, D39*cpsBCD*Δ had only a very small proportion
322 of background positive cells (3.3%), which correlated with its lack of Cps2C (**Figure 7B**).
323 While D39*cpsD*Δ protoplasts had a significant reduction in positive cells compared to the wt
324 (9.5%), this was still greater than that detected for D39*cpsBCD*Δ protoplasts. Interestingly,
325 D39*cpsB*Δ protoplasts showed a significant increase in positive cells. While the lower level
326 of positive D39*cpsD*Δ protoplasts could be attributed to a lower level of CpsC as evidenced
327 by Western immunoblot of insoluble membrane fractions (**Figure 7D**), D39*cpsB* produced
328 similar levels of CpsC to the wt, thus not explaining the increased exposure of the C-terminus
329 to the environment. In order to investigate if this affect was a result of the tyrosine

JB Accepts published online ahead of print

330 phosphatase activity of CpsB, we constructed a mutant in CpsB (D39CpsB$_{H136A}$) lacking
331 tyrosine phosphatase activity(18). Interestingly, this mutation did not have any significant
332 effect on CpsC exposure, suggesting that CpsB role in CpsC topology was independent of its
333 phosphatase activity. TIGR4 protoplasts showed higher Cps4C exposure compared to D39
334 protoplasts (Cps2C) although this did not reach statistical significance (**Figure 7B**).
335
336 We also investigated the surface exposure of CpsC in D39EHA:Cps2C-L11-Cps2D.
337 D39EHA:Cps2C-L11-Cps2D had only 4% positive cells, significantly less than its
338 corresponding wt (D39EHA:Cps2C) and only slightly more than the background 3.3 %
339 positive cells seen in D39*cpsBCD*Δ (**Figure 7C**). This provided further strength to the
340 observation from the CP-B assays, that the fusion of the proteins results in a protein with
341 greatly reduced surface exposed CpsC C-terminus.
342
343
344 **DISCUSSION**
345 CpsC is a major virulence factor of the pneumococcus, crucial via its role in the regulation of
346 the biosynthesis of capsular polysaccharide. For this reason, we set out to investigate its
347 topology, and possible mechanisms it may possess to regulate CpsD BY-kinase activity. Two
348 complementary methods, CP-B accessibility assays and flow cytometry, provided evidence
349 that CpsC topology was not as originally thought, but that the C-terminus of the protein could
350 at least at times be found in an extracellular location. We showed that this phenomenon
351 occurs across pneumococcal strains, as when we performed CP-B accessibility assays with
352 insoluble membrane fractions from TIGR4, cleavage was also detected, with almost complete
353 cleavage at 100 µg/ml. Flow cytometric analysis also detected significant exposure of the C-
354 terminus, with approximately 10% more cells positive in TIGR4 than for D39, thus

JB Accepts published online ahead of print

355 suggesting that Cps2C and Cps4C likely exhibit similar topologies. The slight difference may
356 be due to the fact that Cps2C and Cps4C belong to two different sequence clans (26), and
357 indicating that the C-terminus of Cps4C may be more extracellularly located than Cps2C.
358
359 In order to further investigate this finding, we constructed a strain in which Cps2C was fused
360 to Cps2D via a linker (D39EHA:Cps2C-L11-Cps2D). We hypothesized that this fusion
361 would result in a strain that produces CpsC with its C-terminal region fixed in the cytoplasm,
362 resulting in an altered topology compared to the wt. Indeed, both CP-B accessibility assays
363 (**Figure 5**) and flow cytometry (**Figure 7**), suggested that this was the case.
364 We know that it is critically important that the C-terminus of CpsC interacts with CpsD in
365 order for the BY-kinase to gain functionality (9, 27). For this reason, the C-terminus of CpsC
366 must at least at times be cytoplasmically located. Thus, we hypothesize that the C-terminus of
367 CpsC possesses multiple topologies, at times with the C-termini located within the cytoplasm,
368 at other times extracytoplasmically (**Figure 1B**). We cannot exclude both A and B being
369 present, and that rapid flipping across the membrane occurs. Examples of a variety of
370 membrane proteins across a wide range of genera which possess multiple topologies can be
371 found in the literature (28, 29), and therefore such a finding is not necessarily surprising. It is
372 additionally interesting to speculate that this is a novel method to regulate BY-kinase CpsD
373 activity, and that such a mechanism may be conserved across the majority of Gram-positive
374 bacteria, which possess BY-kinases which are split into two, such as seen in the
375 pneumococcus.
376 Fixing of the CpsC C-terminus into the cytoplasm of *S. pneumoniae* by fusion of CpsC with
377 CpsD did not affect capsule regulation, as has previously been reported (16). This is not
378 particularly surprising, as though we still do not know the detailed mechanism of capsule
379 regulation by this phosphoregulatory system, we do know that cycling between the

JB Accepts published online ahead of print

380 phosphorylated and non-phosphorylated form of the BY-kinase is critical (27). In this fusion
381 strain, switching between phosphorylated and non-phosphorylated CpsD would still occur, as
382 the cognate PTP CpsB acts on the kinase. However, a mutant in the PTP CpsB (D39*cpsB*Δ)
383 showed a significant increase in surface exposed CpsC C-terminus, even though CpsC
384 expression levels were similar to wt. While we initially thought that this may have been due
385 to a loss of phosphatase activity, a mutant which still possesses CpsB but does not have
386 phosphatase activity did not alter CpsC exposure. Thus, this suggests that the structural
387 element of CpsB itself is responsible for this effect. Interestingly, a recent study has
388 suggested that CpsB affects capsule regulation via a mechanism independent of its tyrosine
389 phosphatase activity (18). Further investigation is required to investigate whether CpsB and
390 CpsC specifically interact, and whether this may alter CpsC exposure.
391 It is also important to consider what affects this difference in topology may have on the 3D
392 structure of the protein. While no structure of CpsC has been reported to date, structures of
393 other members of the PCP family have been completed (30). In particular PCP proteins have
394 been shown to form higher order oligomeric structures (FepE – 9, WzzE – 8(30), CapAB -
395 8(27)). Thus, CpsC likely also forms higher oligomers, and change in CpsC topology would
396 likely have significant effects on oligomerization, resulting in functional effects. We are
397 currently working towards a greater structural understanding of CpsC.
398 This study for the first time has described the variable topology of the C-terminus of the PCP
399 and BY-kinase adaptor protein CpsC. The switch between these states is likely critical for the
400 regulation of the activity of the BY-kinase CpsD and subsequent regulation of capsule
401 biosynthesis. With capsule the major virulence factor of the pneumococcus, a greater
402 understanding of its regulation is critical such that we can identify new methods to combat
403 this major human pathogen.
404

405

JB Accepts published online ahead of print

JB Accepts published online ahead of print

406 **Acknowledgements**

407 This study was funded by NHMRC project Grant 1048749 to RM and AS.

408

409 **References**

410 1. **Whitmore, S. E., and R. J. Lamont.** 2012. Tyrosine phosphorylation and bacterial
411 virulence. Int. J. Oral Sci. **4:**1-6.

412 2. **Standish, A. J., A. A. Salim, H. Zhang, R. J. Capon, and R. Morona.** 2012.
413 Chemical inhibition of bacterial protein tyrosine phosphatase suppresses capsule
414 production. PLoS ONE **7:**e36312.

415 3. **Ericsson, D. J., A. Standish, B. Kobe, and R. Morona.** 2012. Wzy-dependent
416 bacterial capsules as potential drug targets. Curr. Drug Targets **13:**1421-1431.

417 4. **Hyams, C., E. Camberlein, J. M. Cohen, K. Bax, and J. S. Brown.** 2010. The
418 *Streptococcus pneumoniae* capsule inhibits complement activity and neutrophil
419 phagocytosis by multiple mechanisms. Infect. Immun. **78:**704-715.

420 5. **Morona, J. K., D. C. Miller, R. Morona, and J. C. Paton.** 2004. The effect that
421 mutations in the conserved capsular polysaccharide biosynthesis genes *cpsA*, *cpsB*,
422 and *cpsD* have on virulence of *Streptococcus pneumoniae*. J. Infect. Dis. **189:**1905-
423 1913.

424 6. **Morona, J. K., R. Morona, D. C. Miller, and J. C. Paton.** 2002. *Streptococcus*
425 *pneumoniae* capsule biosynthesis protein CpsB is a novel manganese-dependent
426 phosphotyrosine-protein phosphatase. J. Bacteriol. **184:**577-583.

427 7. **Morona, J. K., J. C. Paton, D. C. Miller, and R. Morona.** 2000. Tyrosine
428 phosphorylation of CpsD negatively regulates capsular polysaccharide biosynthesis in
429 *Streptococcus pneumoniae*. Mol. Microbiol. **35:**1431-1442.

JB Accepts published online ahead of print

430 8. **Standish, A. J., and R. Morona.** 2014. The role of bacterial protein tyrosine
431 phosphatases in the regulation of the biosynthesis of secreted polysaccharides.
432 Antioxid. Redox. Signal. **20:**2274-2289.
433 9. **Soulat, D., J. M. Jault, B. Duclos, C. Geourjon, A. J. Cozzone, and C.**
434 **Grangeasse.** 2006. *Staphylococcus aureus* operates protein-tyrosine phosphorylation
435 through a specific mechanism. J. Biol. Chem. **281:**14048-14056.
436 10. **Bender, M. H., R. T. Cartee, and J. Yother.** 2003. Positive correlation between
437 tyrosine phosphorylation of CpsD and capsular polysaccharide production in
438 *Streptococcus pneumoniae*. J. Bacteriol. **185:**6057-6066.
439 11. **Morona, R., L. Purins, A. Tocilj, A. Matte, and M. Cygler.** 2009. Sequence-
440 structure relationships in polysaccharide co-polymerase (PCP) proteins. Trends
441 Biochem. Sci. **34:**78-84.
442 12. **Morona, J. K., R. Morona, and J. C. Paton.** 2006. Attachment of capsular
443 polysaccharide to the cell wall of *Streptococcus pneumoniae* type 2 is required for
444 invasive disease. Proc. Natl. Acad. Sci. U. S. A. **103:**8505-8510.
445 13. **Byrne, J. P., J. K. Morona, J. C. Paton, and R. Morona.** 2011. Identification of
446 *Streptococcus pneumoniae* Cps2C Residues That Affect Capsular Polysaccharide
447 Polymerization, Cell Wall Ligation, and Cps2D Phosphorylation. J. Bacteriol.
448 **193:**2341-2346.
449 14. **Purins, L., L. Van Den Bosch, V. Richardson, and R. Morona.** 2008. Coiled-coil
450 regions play a role in the function of the *Shigella flexneri* O-antigen chain length
451 regulator WzzpHS2. Microbiology **154:**1104-1116.
452 15. **Wagner, S., M. M. Klepsch, S. Schlegel, A. Appel, R. Draheim, M. Tarry, M.**
453 **Hogbom, K. J. van Wijk, D. J. Slotboom, J. O. Persson, and J. W. de Gier.** 2008.

JB Accepts published online ahead of print

454 Tuning *Escherichia coli* for membrane protein overexpression. Proc. Natl. Acad. Sci.
455 U. S. A. **105:**14371-14376.
456 16. **Henriques, M. X., T. Rodrigues, M. Carido, L. Ferreira, and S. R. Filipe.** 2011.
457 Synthesis of capsular polysaccharide at the division septum of *Streptococcus*
458 *pneumoniae* is dependent on a bacterial tyrosine kinase. Mol. Microbiol. **82:**515-534.
459 17. **Standish, A. J., U. H. Stroeher, and J. C. Paton.** 2005. The two-component signal
460 transduction system RR06/HK06 regulates expression of *cbpA* in *Streptococcus*
461 *pneumoniae*. Proc. Natl. Acad. Sci. U. S. A. **102:**7701-7706.
462 18. **Geno, K. A., J. R. Hauser, K. Gupta, and J. Yother.** 2014. Streptococcus
463 pneumoniae phosphotyrosine phosphatase CpsB and alterations in capsule production
464 resulting from changes in oxygen availability. J. Bacteriol. **196:**1992-2003.
465 19. **Sung, C. K., H. Li, J. P. Claverys, and D. A. Morrison.** 2001. An rpsL cassette,
466 janus, for gene replacement through negative selection in Streptococcus pneumoniae.
467 Appl. Environ. Microbiol. **67:**5190-5196.
468 20. **Viklund, H., A. Bernsel, M. Skwark, and A. Elofsson.** 2008. SPOCTOPUS: a
469 combined predictor of signal peptides and membrane protein topology.
470 Bioinformatics **24:**2928-2929.
471 21. **Bernsel, A., H. Viklund, A. Hennerdal, and A. Elofsson.** 2009. TOPCONS:
472 consensus prediction of membrane protein topology. Nucleic Acids Res. **37:**W465-
473 468.
474 22. **Hofmann, K., and W. Stoffel.** 1993. Tmbase-A database of membrane-spanning
475 protein segments, p. 166, Biol. Chem. Hoppe-Seyler, vol. 374.
476 23. **Reynolds, S. M., L. Kall, M. E. Riffle, J. A. Bilmes, and W. S. Noble.** 2008.
477 Transmembrane topology and signal peptide prediction using dynamic bayesian
478 networks. PLoS Comput. Biol. **4:**e1000213.

JB Accepts published online ahead of print

479 24. **Byrne, J.** 2012. The role of CpsC in the regulation of *Streptococcus pneumoniae* capsular polysaccharide biosynthesis. Thesis (Ph D). University of Adelaide, School of Molecular and Biomedical Science, 2012.

482 25. **Arrecubieta, C., T. C. Hammarton, B. Barrett, S. Chareonsudjai, N. Hodson, D. Rainey, and I. S. Roberts.** 2001. The transport of group 2 capsular polysaccharides across the periplasmic space in *Escherichia coli*. Roles for the KpsE and KpsD proteins. J. Biol. Chem. **276:**4245-4250.

486 26. **Varvio, S. L., K. Auranen, E. Arjas, and P. H. Makela.** 2009. Evolution of the capsular regulatory genes in *Streptococcus pneumoniae*. J. Infect. Dis. **200:**1144-1151.

489 27. **Olivares-Illana, V., P. Meyer, E. Bechet, V. Gueguen-Chaignon, D. Soulat, S. Lazereg-Riquier, I. Mijakovic, J. Deutscher, A. J. Cozzone, O. Laprevote, S. Morera, C. Grangeasse, and S. Nessler.** 2008. Structural basis for the regulation mechanism of the tyrosine kinase CapB from *Staphylococcus aureus*. PLoS Biol. **6:**e143.

494 28. **Bogdanov, M., and W. Dowhan.** 2012. Lipid-dependent generation of dual topology for a membrane protein. J. Biol. Chem. **287:**37939-37948.

496 29. **Gouffi, K., F. Gerard, C. L. Santini, and L. F. Wu.** 2004. Dual topology of the Escherichia coli TatA protein. J. Biol. Chem. **279:**11608-11615.

498 30. **Tocilj, A., C. Munger, A. Proteau, R. Morona, L. Purins, E. Ajamian, J. Wagner, M. Papadopoulos, L. Van Den Bosch, J. L. Rubinstein, J. Fethiere, A. Matte, and M. Cygler.** 2008. Bacterial polysaccharide co-polymerases share a common framework for control of polymer length. Nat. Struct. Mol. Biol. **15:**130-138.

502

503

504

JB Accepts published online ahead of print

JB Accepts published online ahead of print

505 **Figures Legends**

506 **Figure 1. Topology of CpsC.** (A) Predicted topology of CpsC consisting of two
507 transmembrane domain and one large extracytoplasmic domain, with the N and C-Termini in
508 the cytoplasm as determined by various topology prediction programs detailed in the text.
509 CM represents Cell Membrane (B) Novel topology of CpsC that we predicted based on the
510 results obtained in this study with C-terminus in extra-cytoplasmic location. It is likely that
511 topology flips between A and B.

512

513 **Figure 2. HA-Cps2C in D39EHA:Cps2C is cleaved by CP-B.**

514 (A) Insoluble membrane fractions from *S. pneumoniae* D39EHA:Cps2C were isolated and
515 incubated with indicated concentration of CP-B as described in Materials and Methods.
516 Western immunoblotting using α-HA was used to investigate effect of the protease. A
517 representative immunoblot is shown. (B) Densitometric analysis for each concentration as
518 determined by Image J ($N \geq 3$; Mean ± standard error). At 50 and 100 μg/ ml of CP-B
519 significant cleavage of Cps2C was seen (*** - $p < 0.001$ and **- $p < 0.01$; 2-tailed unpaired *t*
520 test). No degradation products were detectable. (C) Same samples as above were separated on
521 SDS-PAGE and stained with Coomassie Brilliant blue. Protein size is shown in kDa. Arrow
522 indicates the presence of CP-B. (D) In order to identify degradation products, sample
523 concentration was increased by approximately 10 fold and CP-B digestions were separated on
524 16.5 % Tris-tricine gels prior to Western immunoblotting. A degradation product of
525 approximately 9 kDa was identified.

526

527 **Figure 3. Cps4C in TIGR4 is cleaved by CP-B.** (A) Whole cell lysate from *E. coli*
528 Lemo(21) DE3 containing StrepTagII-Cps4C produced a band correlating to the size of CpsC
529 when probed by Western immunoblotting with αCpsCD. (B) Insoluble membrane fractions

JB Accepts published online ahead of print

530 from *S. pneumoniae* TIGR4 were isolated and incubated with indicated concentration of CP-
531 B as described in Materials and Methods. Western immunoblotting using α-CpsCD was used
532 to investigate the protease's effect. A representative immunoblot is shown. (C) Densitometric
533 analysis as determined by Image J (N = 2; Mean ± standard error). 100 µg/ ml of CP-B
534 resulted in almost complete cleavage of Cps4C (** - $p < 0.01$; 2-tailed unpaired *t* test). No
535 degradation products were detectable.
536
537 **Figure 4. HA-Cps2C is cleaved by CP-B in protoplasts.**
538 Protoplasts of D39EHA:Cps2C were produced as described in Methods, and then incubated
539 with CP-B. Protease degradation was detected by Western immunoblotting probing with
540 either (A) αHA to detect degradation of HA:Cps2C or (B) αCpsCD to detect degradation of
541 Cps2D. No degradation of CpsD was detected. (C) Lysed protoplasts of D39EHA:Cps2C
542 were incubated with 100 µg/ ml CP-B and degradation of Cps2D monitored by Western
543 immunoblotting probing with αCpsCD. Almost complete Cps2D degradation was evident.
544 (D) Densitometric analysis of degradation of Cps2C in protoplasts by Image J (N = 3).
545 Significant degradation was seen at 50 and 100 µg/ ml of CP-B (* - $p < 0.05$ and **** -$p <$
546 0.0001; 2-tailed unpaired *t* test).
547
548 **Figure 5. HA:Cps2C-L11-Cps2D is not cleaved by CP-B.**
549 (A) Capsule was prepared from equal numbers of D39EHA:Cps2C (1) and
550 D39EHA:Cps2C-L11-Cps2D (2) of bacterial cells, and capsule level determined as described
551 in Materials and Methods. (B) Whole cell lysates from cells were separated on SDS-PAGE
552 and Western immunoblotting undertaken with αHA, αCpsCD and αPY. Insoluble membrane
553 fractions (C) or protoplasts (D) of D39EHA:Cps2C-L11-Cps2D were incubated with CP-B as
554 described in Materials and Methods and cleavage investigated with Western immunobloting

JB Accepts published online ahead of print

555 probing with αHA. Densitometric analysis using Image J (N ≥ 2; Mean ± standard error),
556 showed that no cleavage occurred (E,F). (G) Solubilized Cps2C-L11-Cps2D from D39 was
557 incubated 100 µg/ml CP-B, and cleavage detected by Western immunoblotting probing with
558 αHA.

559

560 **Figure 6. αCpsCD specifically recognises the C-termini of Cps2C.** Approximately 600µg
561 of D39EHA:CpsC$_{D202\Delta}$ (lane A) and 140µg of D39EHA:Cps2C (lane B) of insoluble fractions
562 were subjected to Western Immunoblotting with either αCpsCD or αHA. While both reacted
563 with HA, only D39EHA:Cps2C reacted with αCpsCD reacted, showing that the antibody
564 only recognises the C-terminus of Cps2C.

565

566 **Figure 7. Flow cytometric analysis of the exposed C-terminus of CpsC.** Flow cytometry
567 of protoplasts from designated strains were investigated as described in Materials and
568 Methods. (A) Representative plot showing D39 (light blue), D39 + no αCpsCD (orange).
569 Positive cell population is indicated (B) CpsC-C terminal positive cells were determined as
570 relative to no αCpsCD control. D39*cpsBCD*Δ and D39*cpsD*Δ were significantly less positive
571 than D39 protoplasts. However, D39*cpsD*Δ produced significantly more positive cells than
572 D39*cpsBCD*Δ. D39*cpsB*Δ displayed enhanced CpsC C-terminus exposure, while a tyrosine
573 phosphatase deficient mutant (D39CpsB$_{H136A}$) showed no difference. (C) Additionally,
574 D39EHA:Cps2C showed significantly greater positive stained cells than D39EHA:Cps2C-
575 L11-Cps2D. (* - $p < 0.05$; ** - $p < 0.01$; *** - $p < 0.001$; Student's 2 tailed t-test). All results
576 represent ≥ 3 replicates (except D39CpsB$_{H136A}$; n = 2) and display Mean ± SE. (D) 10 µg of
577 insoluble membrane fractions of D39, D39*cpsD*Δ and D39*cpsB*Δ were analyzed for CpsC
578 expression by Western immunoblotting with αCpsCD. D39*cpsB*Δ had similar levels of CpsC
579 compared to the wt, while D39*cpsD*Δ showed decreased expression.

JB Accepts published online ahead of print

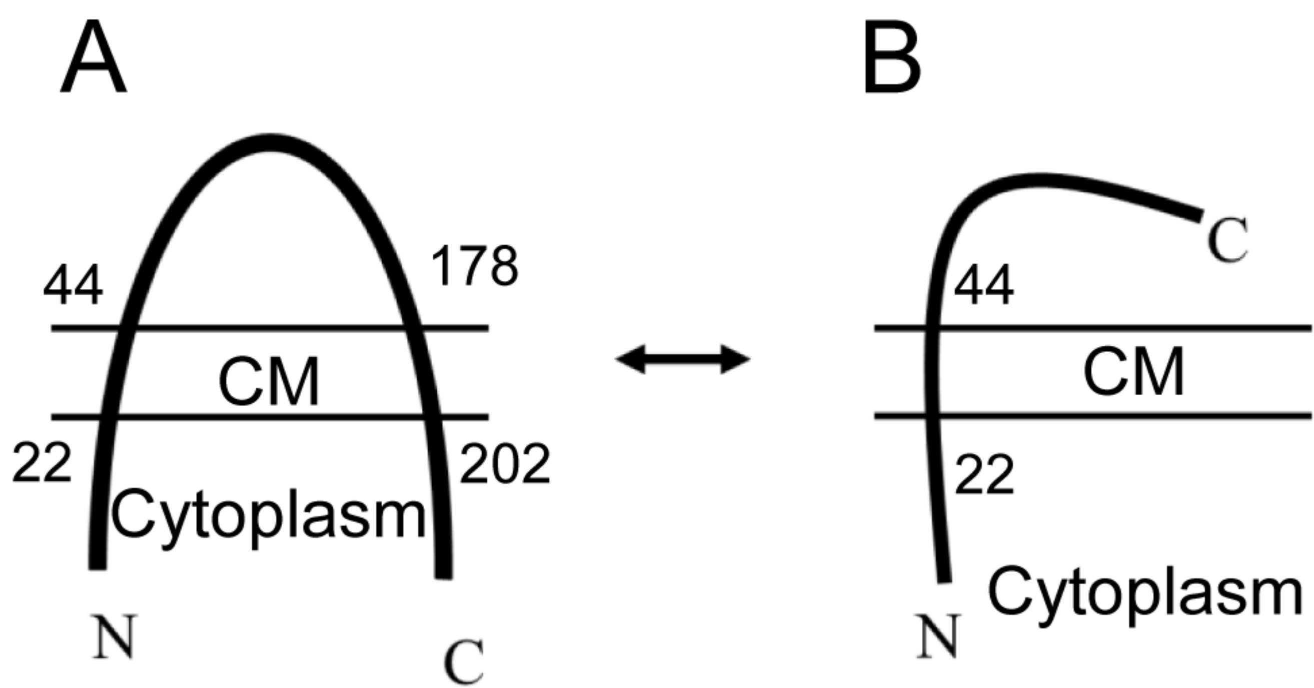

JB Accepts published online ahead of print

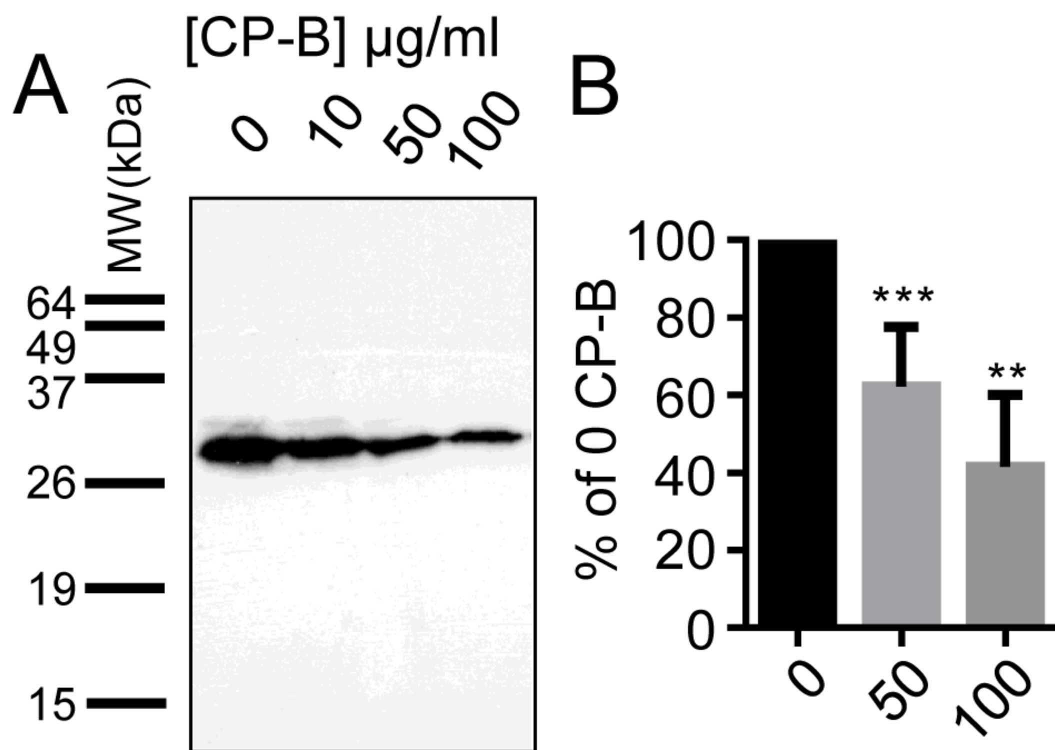

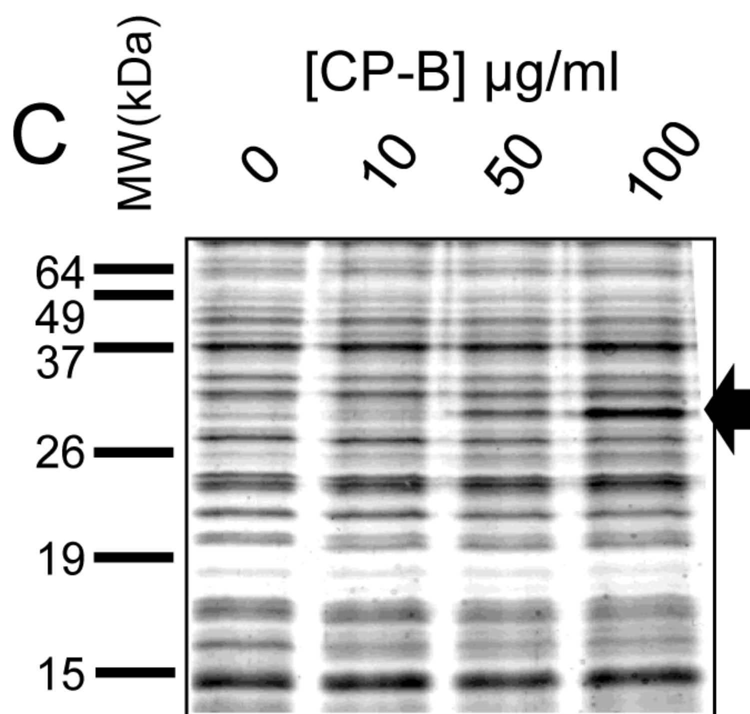

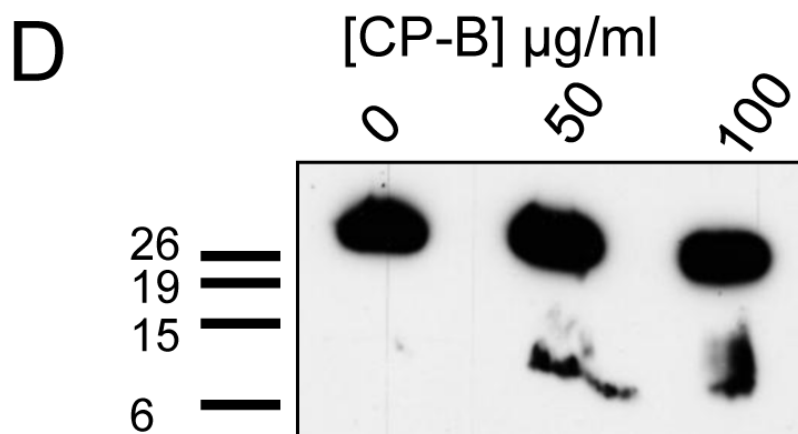

JB Accepts published online ahead of print

A

MW(kDa)

64
49
37
26
19

B

MW(kDa)

[CP-B] µg/ml

0 10 50 100

64
49
37
26
19
15

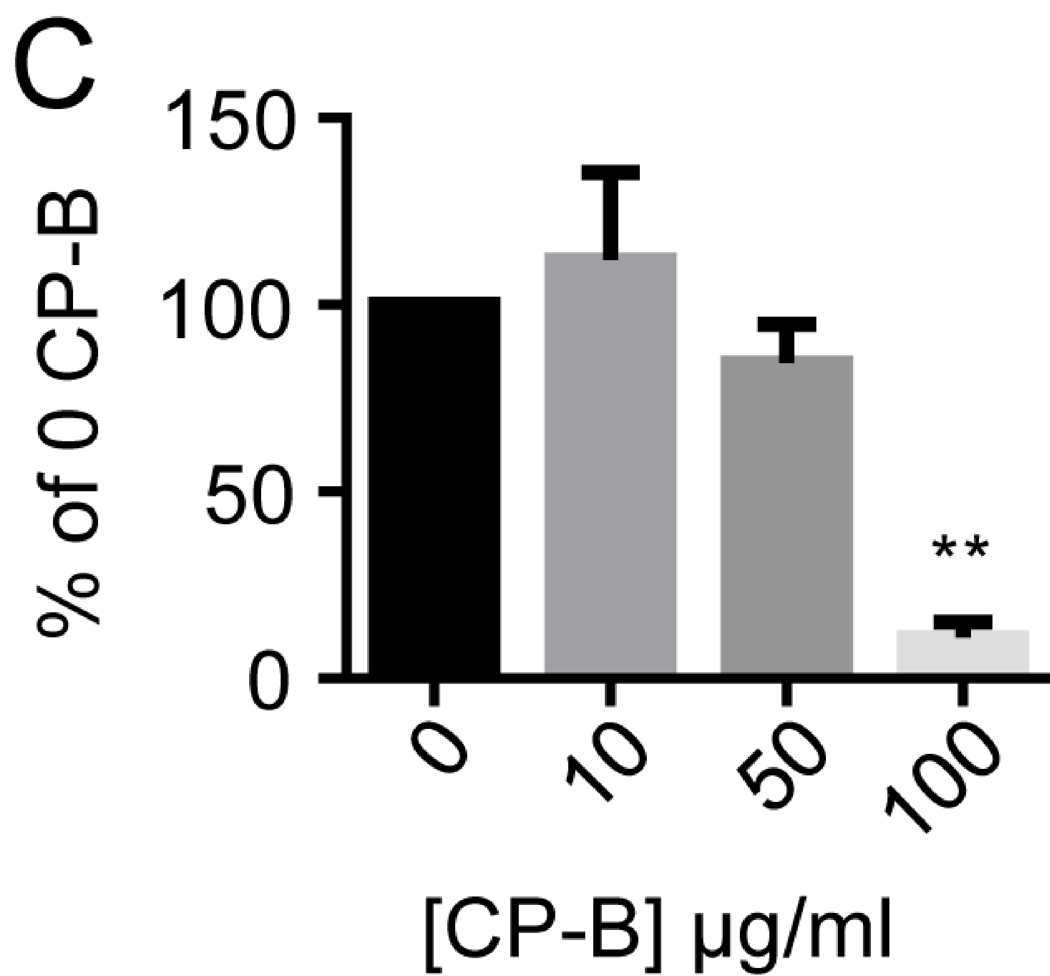

JB Accepts published online ahead of print

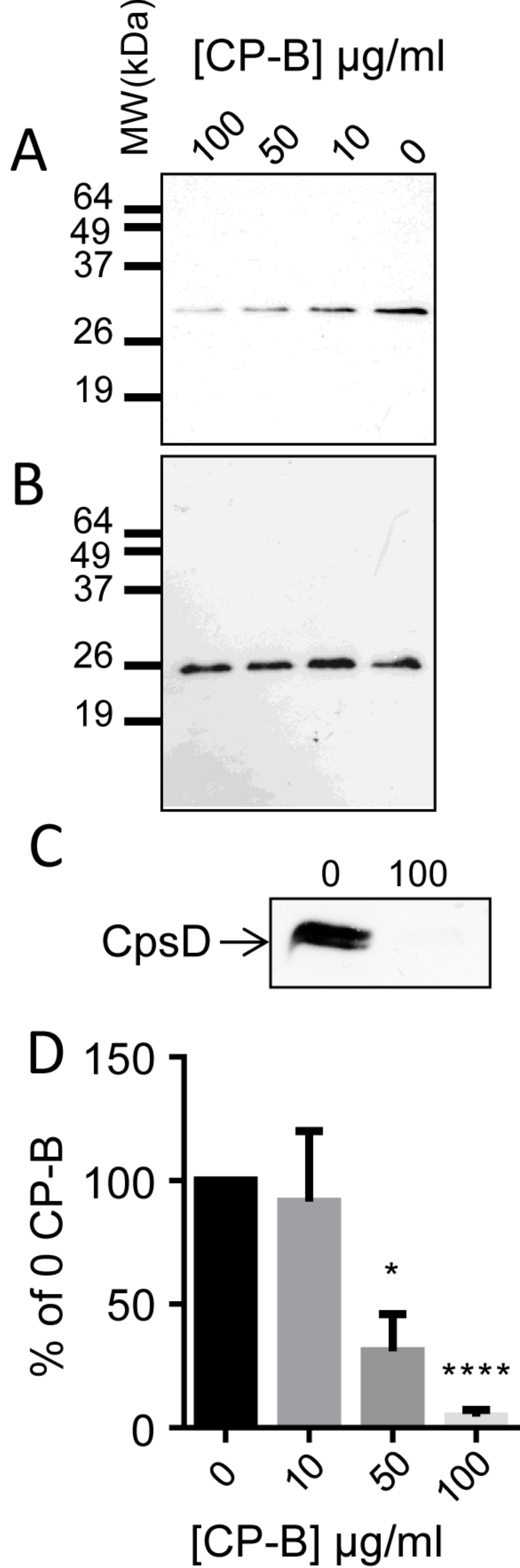

JB Accepts published online ahead of print

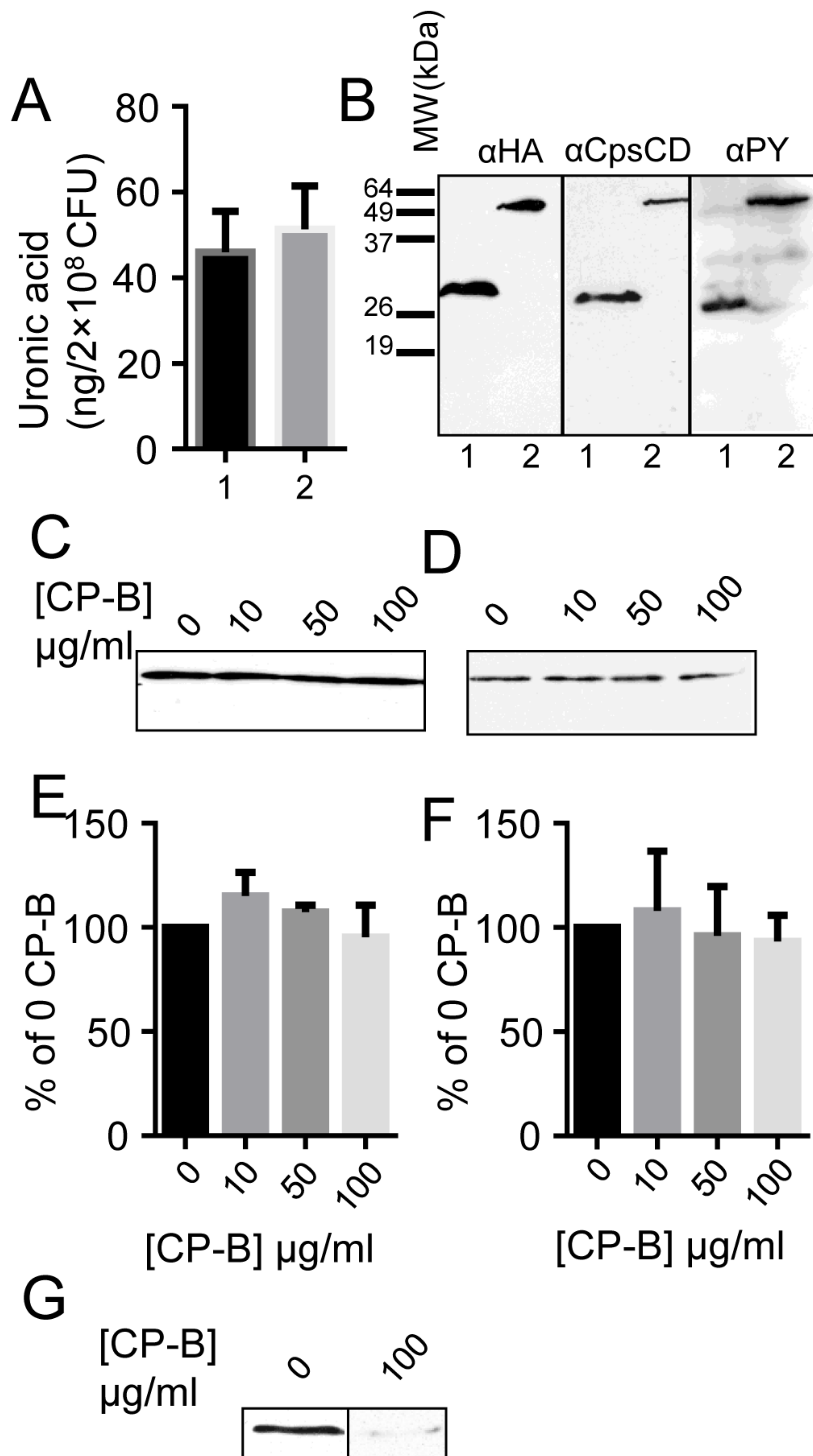

JB Accepts published online ahead of print

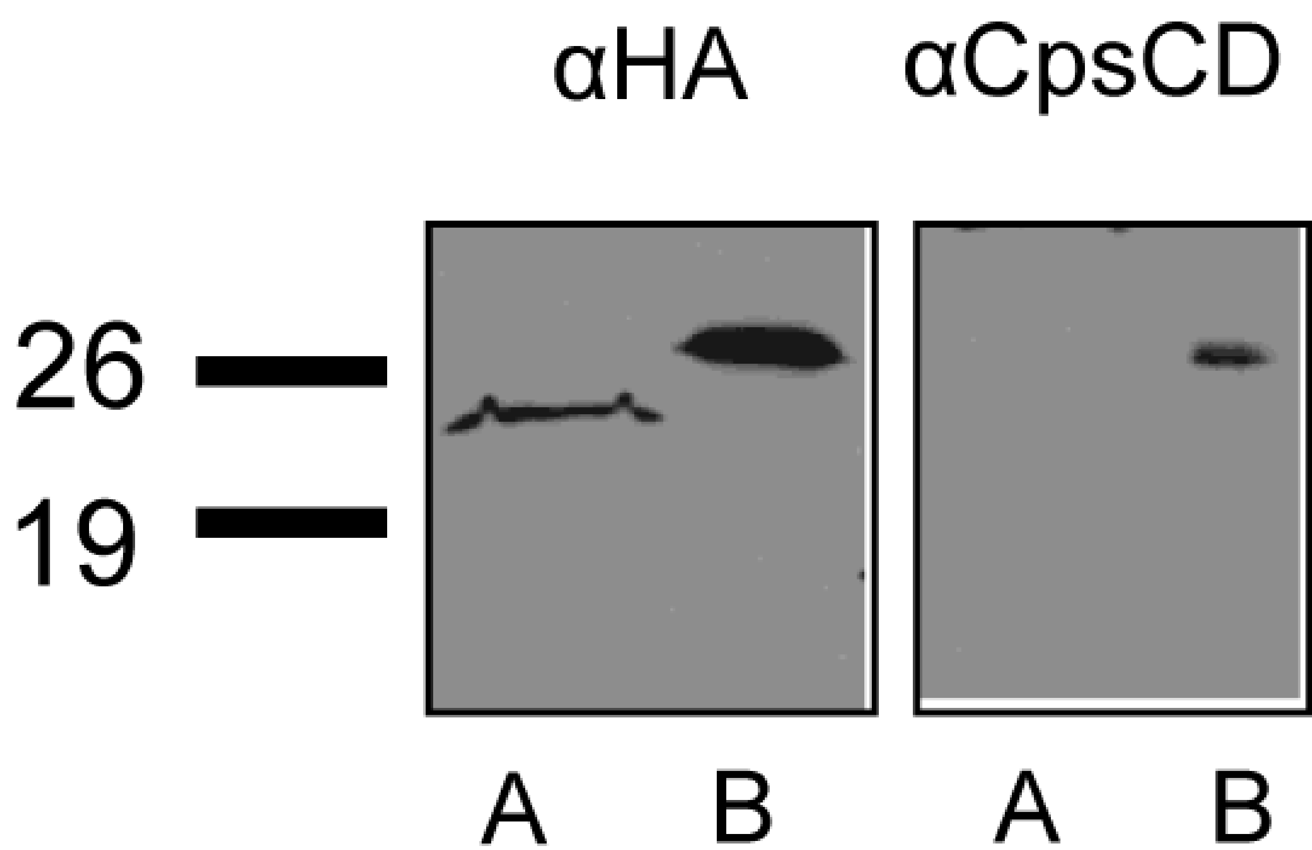

JB Accepts published online ahead of print